

# Simulation Studies of Electron Acceleration to Ultrarelativistic Energies Caused by Small Pulses Generated in Shock Waves

Masatoshi SATO and Yukiharu OHSAWA

*Department of Physics, Nagoya University, Nagoya 464-8602, Japan*

(Received: 29 August 2008 / Accepted: 4 November 2008)

Electron acceleration caused by small pulses in shock waves is studied with relativistic particle simulations. The simulations show that a compressive small pulse generated in a shock wave can accelerate electrons to ultrarelativistic energies. If the external magnetic field is reversed across a neutral sheet, the shock wave creates a field-reversed small pulse, in addition to compressive ones, which also accelerates electrons to ultrarelativistic energies. A theoretical analysis is made on the electron acceleration due to these two types of small pulses. It is confirmed that the simulation results are consistent with the theoretical predictions.

Keywords: shock wave, particle acceleration, high-energy electrons, small pulses, particle simulation

## 1. Introduction

In 1999, it was shown with relativistic, electromagnetic, particle simulations that a shock wave propagating obliquely to an external magnetic field can accelerate electrons to ultrarelativistic energies such that  $\gamma > 100$ , where  $\gamma$  is the Lorentz factor [1]. ( $\gamma \sim 100$  is the energy level of solar energetic electrons [2, 3].) These electrons are reflected near the end of the main pulse region of the shock wave and then accelerated and trapped in the main pulse region. This acceleration occurs when the magnetic field is rather strong,  $|\Omega_e|/\omega_{pe} \gtrsim 1$ , where  $\Omega_e$  and  $\omega_{pe}$  are, respectively, the gyro and plasma frequencies, and is particularly strong if  $v_{sh} \sim c \cos \theta$ , where  $v_{sh}$  is the shock speed and  $\theta$  is the angle between the wave normal and the external magnetic field.

This paper describes another electron acceleration mechanism to ultrarelativistic energies, which is caused by small pulses generated in a shock wave [4–6]. Unlike the above mechanism, this occurs in both strong and weak ( $|\Omega_e|/\omega_{pe} < 1$ ) magnetic fields and does not require the condition  $v_{sh} \sim c \cos \theta$ . In a large-amplitude, magnetosonic shock wave, compressive small pulses, in which the magnetic field is higher than outside, can be generated. Some electrons cross the rear edge of the pulse many times and gain energy from the transverse electric field outside the small pulse [4]; because the pulse is in the shock wave, the electric field is present even outside the pulse. Furthermore, two types of small pulses are generated in a shock wave that passes through a field-reversed region [5, 6]; one is compressive and the other is field-reversed. Some electrons also gain energy from the transverse electric field around the field-reversed small pulse. Simulations show that the Lorentz factors of

accelerated electrons can exceed 100. A theoretical analysis is made on the electron acceleration in these two types of small pulses. It is confirmed that the simulation results are consistent with the theoretical predictions.

In Sec. 2, we outline the acceleration mechanism due to small pulses in a shock wave. We consider two typical motions; gyro and meandering orbits. The former occurs around compressive small pulses, while the latter occurs around field-reversed small pulses. In Sec. 3, we show the results of particle simulations. When the external magnetic field is uniform, a compressive small pulse is generated behind the shock front and accelerates some electrons to ultrarelativistic energies. When the external magnetic field is reversed across a neutral sheet, particle-accelerating compressive and field-reversed small pulses are both generated. We also demonstrate ultrarelativistic acceleration of electrons in such a case. We summarize our work in Sec. 4.

## 2. Electron Motions around Small Pulses

We analyze electron motions around compressive and field-reversed small pulses propagating in the  $x$  direction in an external magnetic field  $\mathbf{B}_0 = (0, 0, B_0)$ . Since we consider the motions of energetic electrons with large gyroradii, we assume that field profiles of small pulses are rectangular [4, 5]. That is,  $\mathbf{B}$  changes from  $(0, 0, B_I)$  to  $(0, 0, B_{II})$ , and  $\mathbf{E}$  from  $(0, E_I, 0)$  to  $(0, E_{II}, 0)$ , at the boundary  $x = x_{bd}$ , which moves with a constant speed (see Fig. 1). Since  $B_z$  and  $E_y$  have similar profiles in a magnetosonic shock wave, the sign of  $E_\lambda/B_\lambda$  is supposed to be positive, where  $\lambda = I$  or  $II$ . In each of the regions (region I and II), particle moves in an ellipse in the momentum space [4]. Some particles stay around the boundary and cross it several

author's e-mail: sato.masatoshi@h.mbox.nagoya-u.ac.jp

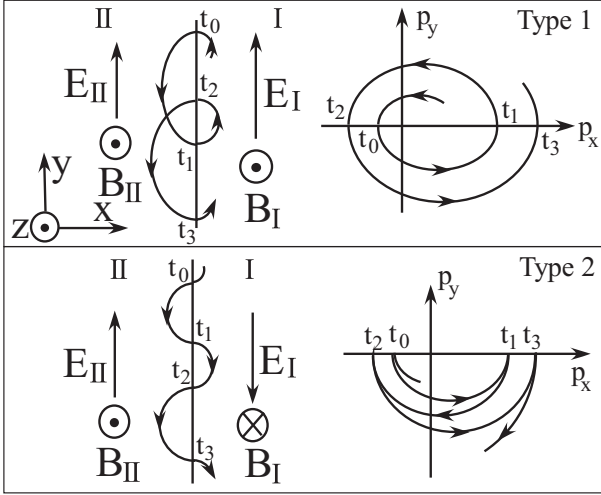


Fig. 1 Schematic diagram of electron orbits in the  $(x, y)$  and  $(p_x, p_y)$  planes. Type 1 and type 2 show the electron motions around compressive and field-reversed small pulses, respectively

times. By connecting the orbits in the two regions, one obtains the orbits of such particles.

Type 1: Compressive small pulse ( $B_I > B_{II} > 0$ ) Since  $B_I > B_{II} > 0$  in this case, the radius of curvature is greater in region II than in region I, and the guiding center of an electron that crosses the boundary many times moves in the negative  $y$  direction, as shown in the upper panel of Fig. 1. The electron gains energy in region II and loses energy in region I. The net energy gain is positive when  $E_{II}/B_{II} > E_I/B_I$ , which leads to the growing of the radius of the ellipse in the momentum space. When  $\gamma \gg 1$ , the Lorentz factor at time  $t_1$  is related to that at  $t = t_0$  through

$$\gamma(t_1) \sim \frac{1 + E_{II}/B_{II}}{1 - E_{II}/B_{II}} \gamma(t_0). \quad (1)$$

Type 2: Field-reversed small pulse ( $B_{II} > 0 > B_I$ ) In this case, the magnetic polarity is reversed at the boundary (lower panel in Fig. 1) and some electrons exhibit meandering motions crossing the neutral sheet,  $x = x_{bd}$ . Their orbits in the momentum space are semi-elliptic in the lower half plane. They gain energy from  $E_{II}$ , and the net energy gain is positive if  $E_{II}/B_{II} > E_I/B_I$ . Equation (1) is valid also in this case [6].

Here, for simplicity, we have described the case of perpendicular wave propagation. This result is, however, applicable to oblique waves if the change in the momentum  $p_z$  is small [4].

### 3. Particle Simulation of Electron Acceleration

We use a one dimensional (one space coordinate and three velocities), relativistic, electromag-

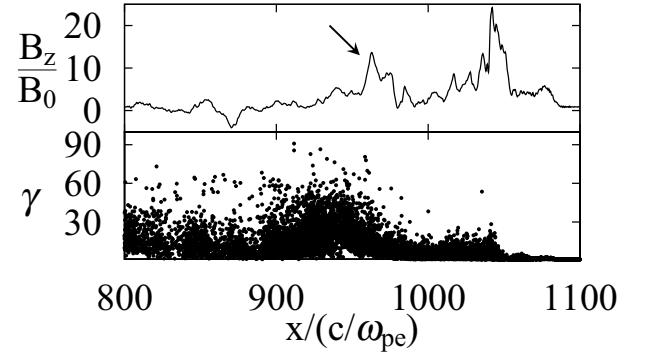


Fig. 2  $B_z$  profile and electron phase space plot  $(x, \gamma)$  at  $\omega_{pe}t = 1100$ . The arrow indicates the compressive small pulse.

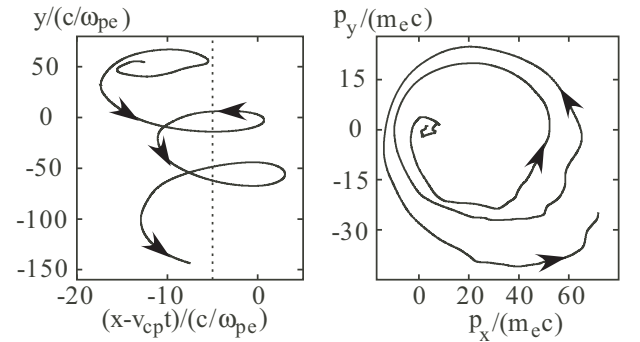


Fig. 3 Orbits of an accelerated electron in the  $(x - v_{cp}, y)$  and  $(p_x, p_y)$  planes. The dotted vertical line in the left panel indicates the rear edge of the compressive small pulse.

netic, particle simulation code with full ion and electron dynamics to study shock waves and associated electron acceleration. The external magnetic field is taken to be rather weak,  $|\Omega|_e/\omega_{pe} = 0.4$ .

#### 3.1 Uniform external magnetic field

First, we show the result of a simulation with a uniform external magnetic field  $\mathbf{B}_0 = B_0(\cos \theta, 0, \sin \theta)$ , where  $\theta$  is taken to be  $60^\circ$ . In this simulation, the compressive small pulse that accelerates electrons is generated only once behind the shock front.

Figure 2 displays the profile of  $B_z$  and phase space plot  $(x, \gamma)$  of electrons at  $\omega_{pe}t = 1100$ . The shock front is at  $x/(c/\omega_{pe}) \sim 1140$  at this time with a propagation speed  $v_{sh} = 18.8v_A$ , where  $v_A$  is the Alfvén speed. Behind the shock front, we find a compressive small pulse (indicated by the arrow), behind which there are ultrarelativistic electrons. The speed of the small pulse is slightly slower than  $v_{sh}$ ; its speed is  $v_{cp} = 15v_A$ .

The left panel of Fig. 3 shows the orbit of an accelerated electron in the  $(x - v_{cp}, y)$  plane for

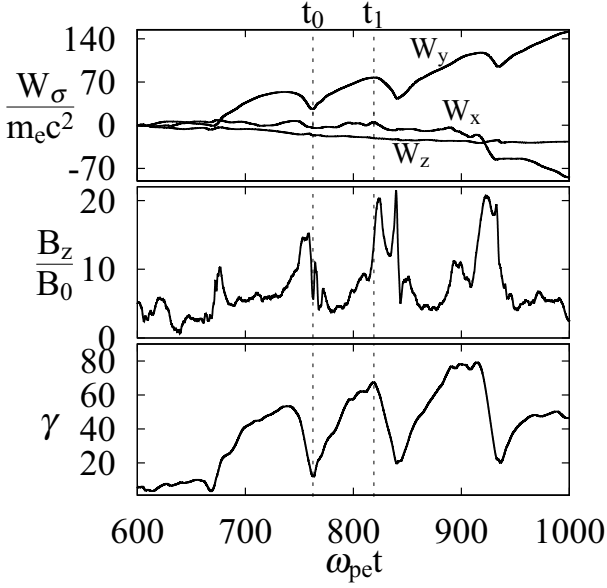


Fig. 4 Time variations of  $W_\sigma$ ,  $B_z$ , and  $\gamma$  of an accelerated electron. The values  $B_z$  are the ones at electron positions.

$600 \leq \omega_{pe}t \leq 900$ . The dotted vertical line indicates the position of the rear edge of the small pulse. This electron stays around the small pulse and crosses its rear edge several times. The right panel exhibits the orbit of this electron in the  $(p_x, p_y)$  plane. The radius of this ellipse-like orbit grows with time. These trajectories in the coordinate and momentum spaces are analogous to the theoretical ones shown in the upper panel of Fig. 1.

In Fig. 4, we plot  $\gamma(t)$  of this particle (bottom panel),  $B_z[x(t)]$  (middle panel), where  $x(t)$  is the position of this particle, and the work done by the electric field (top panel),

$$W_\sigma(t) = -e \int_0^t E_\sigma[x(t)]v_\sigma(t)dt, \quad (2)$$

where the subscript  $\sigma$  denotes  $x$ ,  $y$ , or  $z$ . We find that  $W_y$  and  $\gamma$  of this particle have similar profiles. This indicates that the energy increase is mainly due to transverse electric field  $E_y$ . Furthermore, as mentioned in Sec. 2, the energy of this particle rises when  $B_z$  is weak (the particle is behind the small pulse), while it decreases when  $B_z$  is strong (the particle is in the small pulse).

The theoretical estimate of energy increase is of the same order of magnitude as the simulation result. For instance, the increment of  $\gamma$  from time  $t_0$  to  $t_1$  is  $\delta\gamma = 55$  (see Fig. 4). On the other hand, Eq. (1) gives  $\delta\gamma = 57$ , where for  $E_\Pi$  and  $B_\Pi$  we have used the average values observed in the simulation,

$$\frac{E_\Pi}{B_\Pi} = \int_{t_0}^{t_1} E_\Pi[x(t)]dt / \int_{t_0}^{t_1} B_\Pi[x(t)]dt. \quad (3)$$

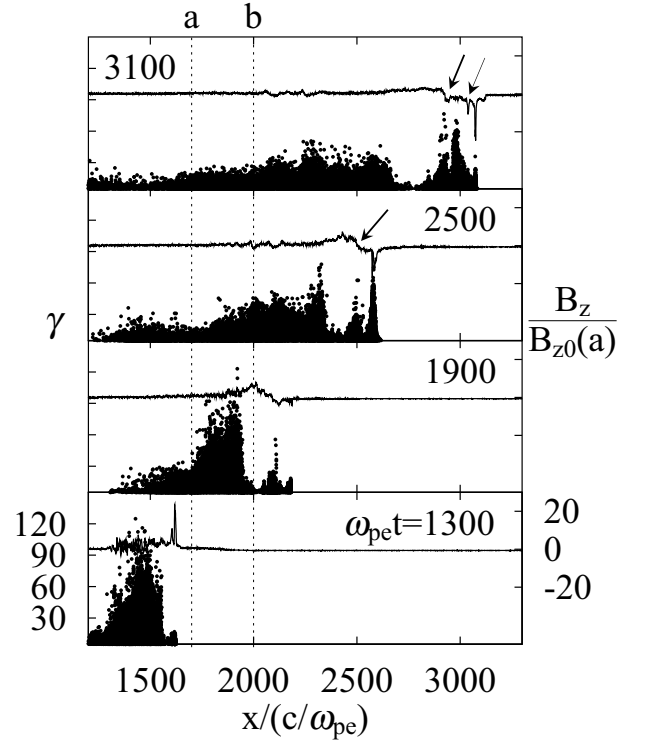


Fig. 5 Phase space plots  $(x, \gamma)$  of electrons and  $B_z$  profiles at various times. The external magnetic field  $B_{z0}$  varies with  $x$  in the region  $a < x < b$  from  $B_{z0}(a)$  to  $B_{z0}(b) = -B_{z0}(a)$ , where  $a/(c/\omega_{pe}) = 1700$  and  $b/(c/\omega_{pe}) = 2000$

The difference between the theoretical and observed values is only 3.6%.

### 3.2 Reversed external magnetic field

Next, we discuss the case in which the external magnetic field  $[0, 0, B_{z0}(x)]$  is reversed. That is,  $B_{z0} (> 0)$  varies from  $B_{z0}(a)$  to  $B_{z0}(b) = -B_{z0}(a)$  in the region  $a < x < b$ . The width  $(b - a)/(c/\omega_{pe})$  is taken to be 300, which is much greater than the width of the shock transition region.

Figure 5 displays  $B_z$  profiles and electron phase space plots  $(x, \gamma)$  at four different times. Here,  $a$  and  $b$  are taken to be  $a/(c/\omega_{pe}) = 1700$  and  $b/(c/\omega_{pe}) = 2000$ ; these positions are indicated by the dotted vertical lines. At  $\omega_{pe}t = 1300$ , an original shock wave, which propagates with a speed  $20.7v_A$ , is in the region  $x < a$ , and thus it has positive  $B_z$ . Behind the original shock wave, there are high-energy electrons. This acceleration is caused by a compressive small pulse; the same mechanism as the one discussed in Sec. 3.1. In the panel of  $\omega_{pe}t = 1900$ , the original shock wave has penetrated into the negative- $B_{z0}$  region, and its amplitude has been damped. At  $\omega_{pe}t = 2500$ , we find that a secondary shock wave, which has negative  $B_z$ , has formed. It propagates with a speed  $20.3v_A$ . In addition, there is a field-reversed small pulse (indicated

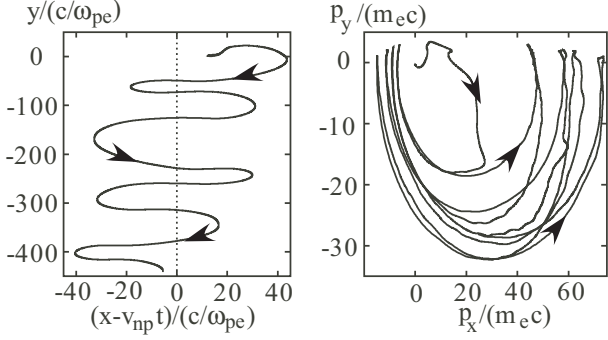


Fig. 6 Orbits of an accelerated electron in the  $(x - v_{np}, y)$  and  $(p_x, p_y)$  planes. The dotted vertical line in the left panel indicates the position of neutral sheet.

by the thick arrow) in the secondary shock wave. The speed of this small pulse is  $v_{np} = 17.9v_A$ . In the panel of  $\omega_{pe}t = 3100$ , a new compressive small pulse has also been generated (indicated by the thin arrow) between the shock front and the field-reversed pulse. In this panel, we find ultrarelativistic electrons behind the new compressive pulse and around the field-reversed pulse.

Figure 6 shows the orbit of an electron accelerated by the field-reversed small pulse in the  $(x - v_{np}, y)$  and  $(p_x, p_y)$  planes for  $1500 \leq \omega_{pe}t \leq 2850$ . The dotted vertical line in the left panel indicates the position of the magnetic neutral sheet. This particle exhibits a meandering motion, crossing the magnetic neutral sheet many times. In the  $(p_x, p_y)$  plane, the orbit of this particle is semi-elliptic in the lower half-plane, with its radius growing with time. These motions are consistent with the theoretical predictions in Sec. 2 (see the lower panel of Fig. 1). It is important to note that there exist transverse electric fields near the magnetic neutral sheet. This occurs because the field-reversed pulse is moving. Meandering electrons gain energy from these transverse electric fields. If the field-reversed configuration is at rest, this type of particle acceleration will not occur [7].

Figure 7 displays the time variations of  $\gamma$ ,  $B_z[x(t)]$ , and  $W_\sigma$  of this electron. The time variation of  $W_y$  is quite similar to that of  $\gamma$ , indicating that this electron absorbs energy from  $E_y$ . In addition, comparison of the curves of  $B_z$  and  $\gamma$  shows that the electron energy increases when  $B_z[x(t)] > 0$  and decreases when  $B_z[x(t)] < 0$ . The increment of  $\gamma$  from time  $t_0$  to  $t_1$  is  $\delta\gamma = 47.7$ . For this time period, Eq. (1) gives  $\delta\gamma = 44.7$ . The difference between the theoretical and observed values is small, 6%.

#### 4. Summary

By using a relativistic electromagnetic particle code, we have studied the electron acceleration mechanism caused by small pulses generated in shock waves.

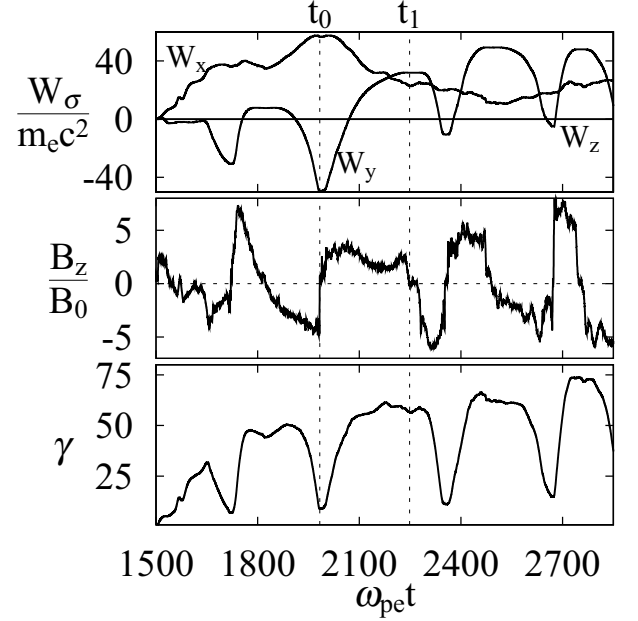


Fig. 7 Time variations of  $W_\sigma$ ,  $B_z$ , and  $\gamma$  of an accelerated electron.

In a uniform external magnetic field, compressive small pulses that accelerate electrons are generated in shock waves. Some electrons cross the rear edge of a compressive pulse many times and gain energy from the transverse electric field behind it.

In a reversed external magnetic field, compressive and field-reversed small pulses that accelerate electrons are generated in a shock wave. After penetrating the reversed field region, the original shock wave is damped. A secondary shock wave with its magnetic polarity opposite to that of the original shock wave is then excited. In this secondary shock wave, particle-accelerating compressive and field-reversed small pulses are generated.

We have also analytically discussed the energization of electrons around these two types of small pulses. The theoretical predictions have accounted for the simulation results of electron acceleration caused by small pulses.

- [1] N. Bessho and Y. Ohsawa, *Phys. Plasmas* **6**, 3076 (1999); *ibid.* **9**, 979 (2002).
- [2] D. J. Forrest and E. L. Chupp, *Nature (London)* **305**, 291 (1983).
- [3] S. R. Kane, E. L. Chupp, D. J. Forrest, G. H. Share, and E. Rieger, *Astrophys. J. Lett.* **300**, L95 (1986).
- [4] M. Sato, S. Miyahara, and Y. Ohsawa, *Phys. Plasmas* **12**, 052308 (2005).
- [5] M. Sato and Y. Ohsawa, *Phys. Plasmas* **13**, 063110 (2006).
- [6] M. Sato and Y. Ohsawa, *J. Phys. Soc. Jpn.* **76**, 104501 (2007); *ibid.* **77**, 084502 (2008).
- [7] E. G. Harris, *Nuovo Cimento* **23**, 115 (1962).